LETTERS

RAG2 PHD finger couples histone H3 lysine 4 trimethylation with V(D)J recombination

Adam G. W. Matthews[1]*, Alex J. Kuo[2]*, Santiago Ramón-Maiques[3], Sunmi Han[1], Karen S. Champagne[4], Dmitri Ivanov[5], Mercedes Gallardo[1], Dylan Carney[2], Peggie Cheung[2], David N. Ciccone[1], Kay L. Walter[2], Paul J. Utz[6], Yang Shi[7], Tatiana G. Kutateladze[4], Wei Yang[3], Or Gozani[2]* & Marjorie A. Oettinger[1]*

Nuclear processes such as transcription, DNA replication and recombination are dynamically regulated by chromatin structure. Eukaryotic transcription is known to be regulated by chromatin-associated proteins containing conserved protein domains that specifically recognize distinct covalent post-translational modifications on histones. However, it has been unclear whether similar mechanisms are involved in mammalian DNA recombination. Here we show that RAG2—an essential component of the RAG1/2 V(D)J recombinase, which mediates antigen-receptor gene assembly[1]—contains a plant homeodomain (PHD) finger that specifically recognizes histone H3 trimethylated at lysine 4 (H3K4me3). The high-resolution crystal structure of the mouse RAG2 PHD finger bound to H3K4me3 reveals the molecular basis of H3K4me3-recognition by RAG2. Mutations that abrogate RAG2's recognition of H3K4me3 severely impair V(D)J recombination *in vivo*. Reducing the level of H3K4me3 similarly leads to a decrease in V(D)J recombination *in vivo*. Notably, a conserved tryptophan residue (W453) that constitutes a key structural component of the K4me3-binding surface and is essential for RAG2's recognition of H3K4me3 is mutated in patients with immunodeficiency syndromes. Together, our results identify a new function for histone methylation in mammalian DNA recombination. Furthermore, our results provide the first evidence indicating that disrupting the read-out of histone modifications can cause an inherited human disease.

Many studies suggest that V(D)J recombination is regulated by modulating the chromatin structure of antigen-receptor loci during lymphoid development[2]. Several studies have analysed the pattern of histone modifications present at the immunoglobulin heavy chain locus during B-cell development[3–5]. However, mechanisms linking histone modifications to the function of the RAG recombinase have remained elusive.

Because RAG2 contains a non-canonical plant homeodomain (PHD) finger[6,7]—a module that can mediate interactions with chromatin[8–10]—we asked whether a polypeptide encompassing the RAG2 PHD finger ($RAG2_{PHD}$; amino acids 414–527) can recognize modified histone proteins. In an *in vitro* screen of peptide microarrays containing ~70 distinct modified histone peptides, we found that $RAG2_{PHD}$ specifically binds to histone H3 trimethylated at lysine 4 (H3K4me3) (Fig. 1a, Supplementary Fig. 1, and data not shown). The specificity of this interaction was confirmed by peptide pull-down assays (Fig. 1b, Supplementary Fig. 2 and Supplementary Fig. 3). RAG2 has a carboxy-terminal extension of 40 amino acids that is essential for phosphoinositide (PtdIns)-binding[7] (amino acids 488–527), but this region is dispensable for H3K4me3-binding because the minimal PHD finger alone (amino acids 414–487) is sufficient for H3K4me3-recognition (Fig. 1c). In addition, the acidic hinge region of RAG2 (amino acids 388–412), previously implicated in histone-binding[11], is dispensable for recognition of H3K4me3 (Fig. 1d). Moreover, mutations in the acidic hinge region, which had previously been shown to interfere with histone binding[11], had no effect on the H3K4me3 interaction (Fig. 1d). Using calf thymus histone protein pull-down assays, we confirmed that the interaction between $RAG2_{PHD}$ and H3K4me3 occurs in the context of full-length histone proteins (Fig. 1e). Furthermore, $RAG2_{PHD}$ bound to native mononucleosomes purified from HeLa cells, but not to mononucleosomes reconstituted from bacterially expressed recombinant histones, indicating that the $RAG2_{PHD}$–nucleosome interaction is dependent on post-translational histone modifications (Fig. 1f). Although full-length RAG2 binds H3K4me3 peptides, core RAG2 (amino acids 1–387)—the minimal portion of RAG2 required for V(D)J cleavage *in vitro*—which lacks the PHD finger, does not (Fig. 1g). Consistent with the pull-down results, tryptophan fluorescence measurements using $RAG2_{PHD}$ determined dissociation constants (K_d) of ~4 μM for H3K4me3, ~60 μM for H3K4me2, ~120 μM for H3K4me1 and ~500 μM for H3K4me0 (Supplementary Fig. 5). Thus, the RAG2 PHD finger is a chromatin-binding module that recognizes H3K4me3.

To understand the molecular basis of the interaction between the RAG2 PHD finger and H3K4me3, we determined the crystal structure of the $RAG2_{PHD}$–H3K4me3 complex at 1.15 Å resolution (Fig. 2, Supplementary Fig. 6 and Supplementary Table 1). In three previously published PHD–H3K4me3 structures[12–14], the H3 peptide extends straight through the peptide-binding groove. However, in the $RAG2_{PHD}$–H3K4me3 structure, the H3 peptide is kinked by ~90° at Q5. The K4me3 side chain is recognized by cation–π interactions within an aromatic channel delimited by Y415 on the left, M443 on the back and W453 on the right (Fig. 2a). Despite not revealing any primary sequence conservation with the K4me3-binding residues of ING2, BPTF and YNG1 (Supplementary Fig. 7), RAG2 forms a similar K4me3-binding pocket (Fig. 2c). Interestingly, $RAG2_{PHD}$ lacks the canonical 'aromatic cage' often employed to bind trimethylated lysine residues[15] (Fig. 2b, c). Instead of being closed on both sides, the back and the top (as observed with other PHD fingers[12–14]), the $RAG2_{PHD}$ K4me3-binding surface is open on the top, and resembles an 'aromatic

[1]Department of Molecular Biology, Massachusetts General Hospital and Department of Genetics, Harvard Medical School, Boston, Massachusetts 02114, USA. [2]Department of Biological Sciences, Stanford University, Stanford, California 94305, USA. [3]Laboratory of Molecular Biology, NIDDK, NIH, Bethesda, Maryland 20892, USA. [4]University of Colorado Health Sciences Center, Aurora, Colorado 80045, USA. [5]Department of Biological Chemistry and Molecular Pharmacology, Harvard Medical School, Boston, Massachusetts 02115, USA. [6]Department of Medicine, Stanford University School of Medicine, Stanford, California 94305, USA. [7]Department of Pathology, Harvard Medical School, Boston, Massachusetts 02115, USA.
*These authors contributed equally to this work.

channel' rather than an 'aromatic cage' (Fig. 2b, c). This 'channel' conformation may provide a mechanism to modulate histone binding[16]. Aside from the K4me3 and Q5 residues, the remaining side chains of H3 form no specific interactions with $RAG2_{PHD}$. Finally, unlike other H3K4me3-binding PHD fingers[9,12–14,17], $RAG2_{PHD}$ does not have acidic residues (Asp or Glu) positioned to electrostatically interact with H3R2 (ref. 16) (Fig. 2c).

The three residues in RAG2 that form the aromatic channel critical for trimethyl-lysine recognition are completely conserved through evolution (Supplementary Fig. 8). As expected, mutating any one of these residues (Y415A, M443A, W453A/R) abrogated H3K4me3-binding by $RAG2_{PHD}$ (Fig. 3a) and by full-length RAG2 (Fig. 3b). Because the W453R mutation has been implicated in the pathogenesis of Omenn's syndrome[18]—a rare severe combined immunodeficiency[19]—and the molecular mechanism linking this mutation to Omenn's syndrome remains unknown[7], we further characterized W453R's role in histone binding. Consistent with the critical role of this residue in forming the recognition surface for H3K4me3, introducing this mutation into the RAG2 PHD finger ($RAG2_{PHD\text{-}W453R}$) abolished the ability of $RAG2_{PHD}$ to bind either full-length histone H3 (Fig. 3c) or intact nucleosomes (Fig. 3d). Thus, the interaction of RAG2 with histone proteins *in vitro* is dependent on H3K4me3-binding. We note that $RAG2_{PHD\text{-}W453R}$ is properly folded, as indicated by a comparison of the ^{1}H-^{15}N heteronuclear single quantum correlation spectra of $RAG2_{PHD}$ and $RAG2_{PHD\text{-}W453R}$ (Supplementary Fig. 9). In addition, the Y415A and M443A substitutions had no effect on PtdIns-binding by $RAG2_{PHD}$ (Supplementary Fig. 10), and W453R-associated recombination defects were previously demonstrated to be independent of the PtdIns-binding activity of RAG2 (ref. 7). Thus, the identification of multiple different point mutations that selectively abrogate RAG2's recognition of H3K4me3 allowed us to study the functional significance of this interaction.

Before analysing the effect of H3 methylation on V(D)J recombination *in vivo*, we first wanted to confirm that $RAG2_{Y415A}$, $RAG2_{M443A}$ and $RAG2_{W453R}$ disrupt H3K4me3-binding without affecting protein folding or the inherent catalytic properties of RAG2. We tested the ability of recombinant wild-type and mutant RAG2 proteins to catalyse V(D)J cleavage *in vitro* on a naked DNA substrate. In these assays, the recombinant proteins, which all expressed and purified equally well (Fig. 3e), were incubated with core RAG1 (amino acids 384−1008), and a DNA substrate. All three H3K4me3-binding mutants catalysed V(D)J cleavage at wild-type levels (Fig. 3f). Therefore, the H3K4me3-binding mutants—$RAG2_{Y415A}$, $RAG2_{M443A}$ and $RAG2_{W453R}$—are properly folded and catalytically active and, thus, can be used for *in vivo* functional analyses.

Next, to address whether the recognition of methylated H3 by $RAG2_{PHD}$ has a role in regulating RAG2 function *in vivo*, we performed extrachromosomal V(D)J recombination assays with the H3K4me3-binding mutants. Fibroblast cell lines were transfected with an exogenous recombination substrate that becomes partially chromatinized when introduced into cells and that has nucleosomes positioned over the recombination signal sequences[20], along with full-length RAG1, and either full-length wild-type RAG2, $RAG2_{Y415A}$, $RAG2_{M443A}$, or $RAG2_{W453R}$. Strikingly, despite being expressed at comparable levels to wild-type RAG2 (Fig. 4a, western blot), all three H3K4me3-binding mutants exhibited a profound decrease (>90%) in recombination activity (Fig. 4a, graph). Thus, the H3K4me3-recognition activity of RAG2 is required for V(D)J recombination *in vivo*.

To test directly the importance of H3K4 methylation and the interaction between RAG2 and H3K4me3 for V(D)J recombination *in vivo*, we used two different methods to reduce endogenous H3K4 methylation levels, and then repeated the extrachromosomal V(D)J recombination assays. First, H3K4 methylation levels were reduced (Fig. 4b, western blot) by knocking down expression of the common histone H3 lysine 4 methyltransferase component WDR5 (refs 15 and 21) with short hairpin (sh)RNA. Consistent with the decreased

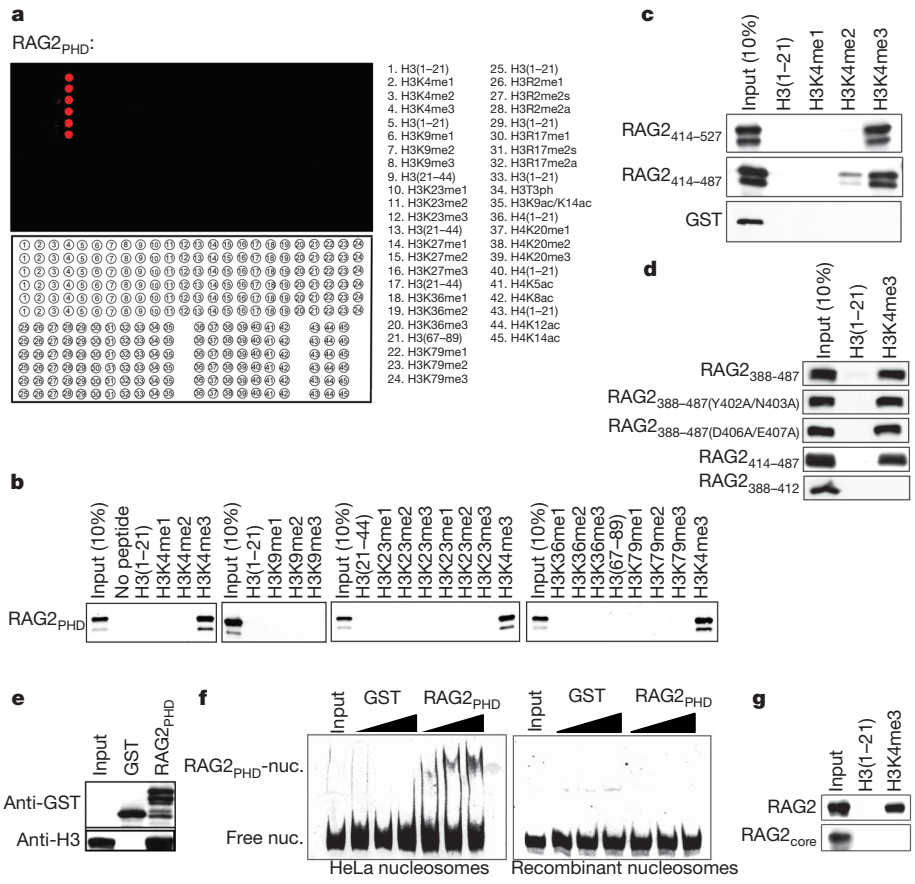

Figure 1 | The RAG2 PHD finger is a novel H3K4me3-binding module. **a**, $RAG2_{PHD}$ preferentially binds H3K4me3 peptides. Peptide microarrays containing the indicated histone peptides were probed with glutathione *S*-transferase (GST)–$RAG2_{414–527}$ ($RAG2_{PHD}$). Red spots indicate peptide binding by $RAG2_{PHD}$. The integrity of peptides was previously confirmed[9,17] (Supplementary Fig. 4). H3, histone H3; H4, histone H4; me, methylation; ac, acetylation; ph, phosphorylation; s, symmetric; a, asymmetric. **b**, Western blot analysis of histone peptide pull downs with $RAG2_{PHD}$ and indicated biotinylated peptides. **c**, $RAG2_{414–487}$ is sufficient for recognition of H3K4me3 in a histone peptide pull-down assay, as in **b**. GST alone is shown as a negative control. **d**, The RAG2 hinge region (amino acids 388–412) is dispensable for H3K4me3-recognition. Peptide pull-down assays as in **b**, with the indicated proteins. **e**, A western blot of $RAG2_{PHD}$ and GST control pull downs from calf thymus histones. **f**, A gel-shift assay comparing $RAG2_{PHD}$ binding to purified native HeLa nucleosomes (left panel) or nucleosomes reconstituted from recombinant, bacterially expressed histone proteins (right panel). Ethidium-bromide stain of nucleosomal DNA on a non-denaturing polyacrylamide gel. **g**, Full-length RAG2, but not $RAG2_{core}$ recognizes H3K4me3. Peptide pull-down assays as in **b**, with the indicated proteins.

recombination observed with the H3K4me3-binding mutants, we observed a marked reduction in the recombination activity of wild-type RAG2 (~60%) in cells carrying the *WDR5* shRNA (Fig. 4b, table and left graph). Significantly, V(D)J recombination by $RAG2_{W453R}$—which does not recognize H3K4me3—was unaffected by the presence of *WDR5* shRNA (Fig. 4b, table and right graph), indicating that the reduction observed for wild-type RAG2 is specifically due to reduced H3K4me3 binding. In a second independent method, we reduced H3K4me3 levels by transiently expressing the H3K4me3 demethylase SMCX (also known as JARID1C)[22]. As with *WDR5* shRNA, we observed that decreases in H3K4me3 levels (Fig. 4c, western blot) resulted in a significant reduction in recombination (~45%) in cells expressing SMCX (Fig. 4c, table and left graph). V(D)J recombination by $RAG2_{W453R}$ was unaffected by SMCX expression (Fig. 4c, table and right graph). Thus, reducing either the levels of H3K4 methylation or the ability of RAG2 to bind H3K4me3, impairs V(D)J recombination.

Because H3K4me3 is observed at actively rearranging gene segments[23] (Supplementary Fig. 12), we assayed the ability of the H3K4me3-binding mutants to perform chromosomal V(D)J recombination at the endogenous murine IgH locus. $RAG2^{-/-}$ Pro-B cells were transduced with lentiviruses encoding either RAG2, $RAG2_{Y415A}$, $RAG2_{M443A}$ or $RAG2_{W453R}$ and the extent of D_H-to-J_H recombination in the transduced cell populations was measured using a standard semi-quantitative PCR strategy. Despite being expressed at comparable levels to wild-type RAG2 (Fig. 4d, left panel), all three H3K4me3-binding mutants exhibited a dramatic reduction in D_H-to-J_H recombination (Fig. 4d, right panel). Thus, we conclude that recognition of H3K4me3 by $RAG2_{PHD}$ is crucial for V(D)J recombination at the endogenous immunoglobulin locus.

Our findings provide the first direct molecular link between histone methylation and mammalian DNA recombination. Before this study, H3K4me3 had only been demonstrated to function in the regulation of gene expression[15]. Our results, demonstrating a novel function for this mark in V(D)J recombination, highlight that chromatin structure can be coupled to diverse nuclear processes by protein modules that recognize modified histones. We have also provided the first evidence that disrupting the read-out of histone modifications can cause an inherited human disease. Omenn's syndrome has been observed in patients carrying a W453R mutation in RAG2 (ref. 18). Because $RAG2_{W453R}$ exhibits wild-type enzymatic activity *in vitro*[7] (Fig. 3f), it has been unclear how this mutation causes immunodeficiency. Here we have shown that the W453R mutation disrupts the read-out of H3K4me3, thereby providing a molecular explanation of how $RAG2_{W453R}$ causes Omenn's syndrome. Although the W453R,

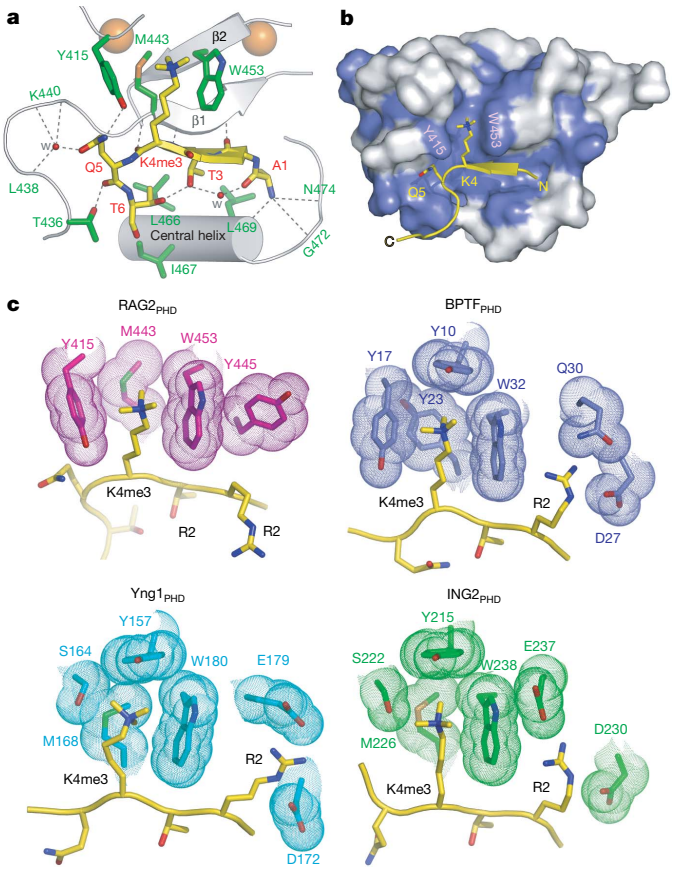

Figure 2 | The molecular basis of H3K4me3-recognition by $RAG2_{PHD}$. **a**, **b**, A 1.15 Å crystal structure of $RAG2_{414–487}$ complexed with H3K4me3 peptide. **a**, Ribbon diagram of the complex. For clarity, only the central portion of $RAG2_{414–487}$ is shown (silver). Residues with side chains that interact with the H3 peptide are shown as green sticks with blue (nitrogen) and red (oxygen) highlights. Residues with main chain atoms that interact with the peptide are labelled in green. The peptide is shown in yellow. With the exception of R2, the side chains of A1 to T6 all interact with RAG2 and are shown in stick models. Zn^{2+} ions are shown as orange spheres and water molecules mediating protein–peptide interactions are shown as red spheres. Grey dashed lines represent hydrogen bonds. $RAG2_{PHD}$ consists of two unorthodox, interdigitated zinc fingers, linked by a pair of anti-parallel β-strands and a central α-helix. The backbone of residues two–four of the histone H3 peptide are hydrogen-bonded, with one of the β-strands of $RAG2_{PHD}$ forming a 3-stranded antiparallel β-sheet. **b**, The H3 peptide binding surface is conserved among RAG2 proteins. Residues of RAG2 that are conserved through evolution (see Supplementary Fig. 5) are coloured blue on the molecular surface. **c**, Structural comparison of the PHD fingers from murine RAG2, human BPTF, yeast Yng1 and murine ING2. Side chains in the PHD fingers that interact with H3K4me3 and H3R2 are highlighted with molecular surface.

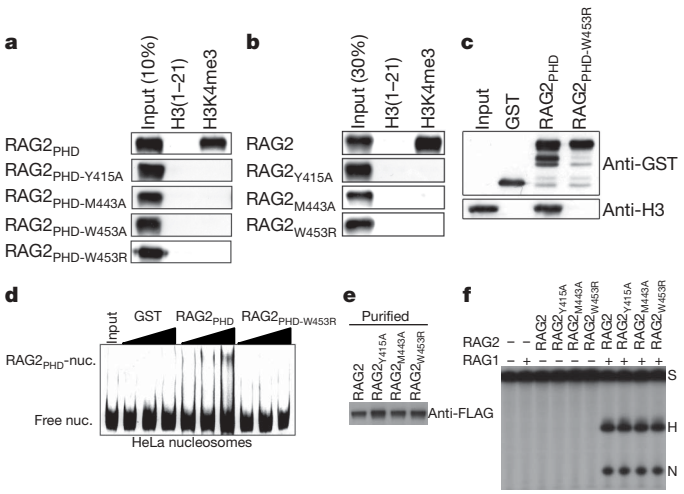

Figure 3 | Recognition of H3K4me3 by $RAG2_{PHD}$ is dispensable for RAG2 *in vitro* enzymatic activity, but essential for RAG2 binding to native histones. **a**, Identification of RAG2 PHD finger mutations that specifically disrupt H3K4me3-recognition. Western blot analysis of histone peptide pull downs, with the indicated GST fusion proteins and biotinylated peptides. **b**, $RAG2_{PHD}$ mutations specifically disrupt binding of full-length RAG2 to H3K4me3. Western blot analysis of histone peptide pull downs with wild-type and mutant full-length RAG2 proteins and the indicated biotinylated histone peptides. **c**, The interaction of RAG2 with histone H3 is dependent on H3K4me3 binding. Western analysis of GST–$RAG2_{PHD}$, GST–$RAG2_{PHD-W453R}$, and GST control pull downs from calf thymus histones. **d**, The interaction of RAG2 with native nucleosomes requires H3K4me3-binding activity. Nucleosome-binding assays as in Fig. 1f with wild-type ($RAG2_{PHD}$) and mutant ($RAG2_{PHD–W453R}$) GST-fusion proteins. **e**, Wild-type and mutant RAG2 proteins express and purify equally well. Anti-Flag western analysis of the indicated Flag-tagged full-length RAG2 proteins purified from 293T cells. **f**, Mutant RAG2 proteins catalyse wild-type V(D)J cleavage *in vitro*. The indicated recombinant proteins were tested for *in vitro* V(D)J cleavage activity. The positions of the substrate (S) and cleavage products (hairpin (H) and nick (N)) are indicated.

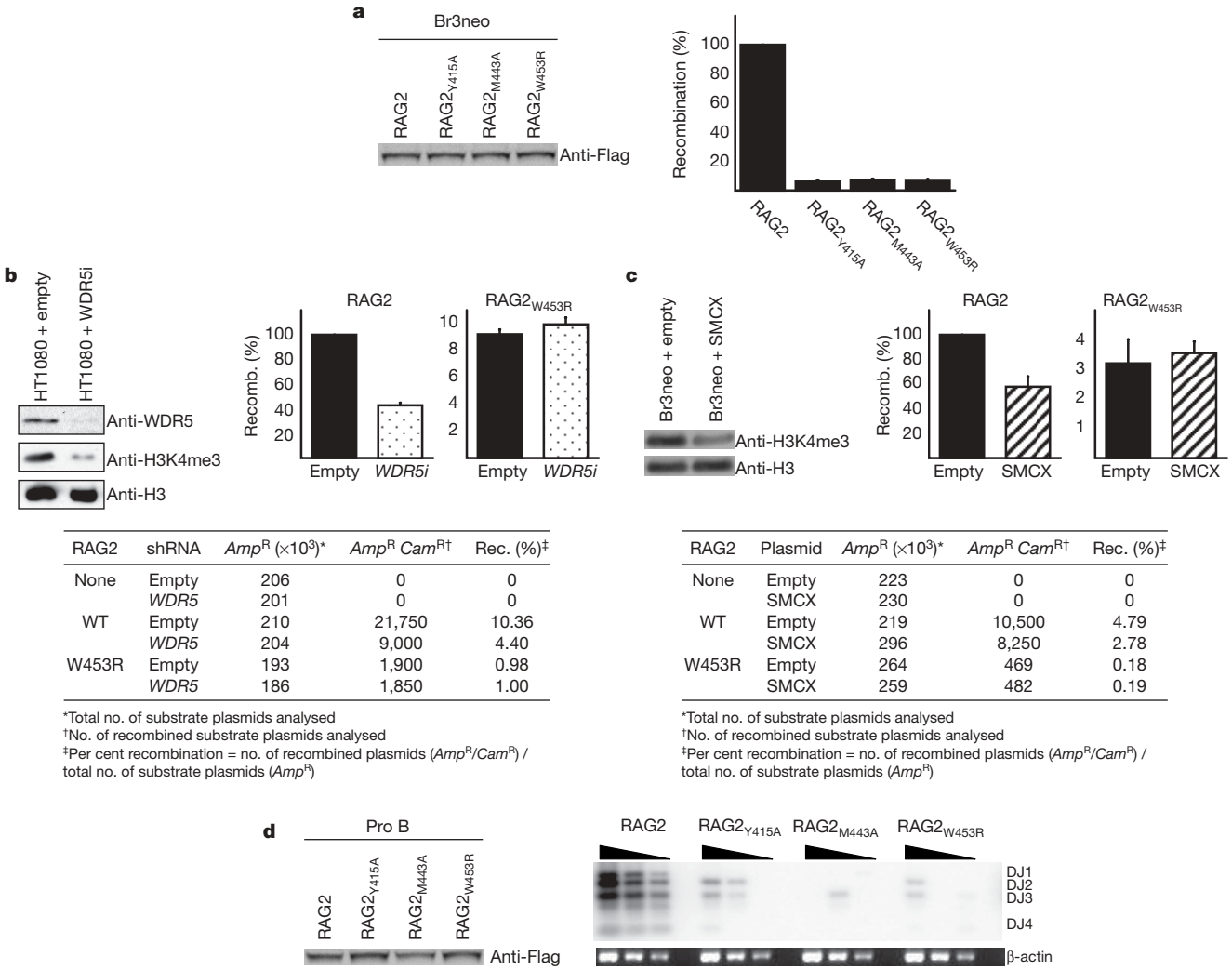

RAG2	shRNA	*Amp*^{R} (×10^3)*	*Amp*^{R} *Cam*^{R}†	Rec. (%)‡
None	Empty	206	0	0
	WDR5	201	0	0
WT	Empty	210	21,750	10.36
	WDR5	204	9,000	4.40
W453R	Empty	193	1,900	0.98
	WDR5	186	1,850	1.00

*Total no. of substrate plasmids analysed
†No. of recombined substrate plasmids analysed
‡Per cent recombination = no. of recombined plasmids (*Amp*^{R}/*Cam*^{R}) / total no. of substrate plasmids (*Amp*^{R})

RAG2	Plasmid	*Amp*^{R} (×10^3)*	*Amp*^{R} *Cam*^{R}†	Rec. (%)‡
None	Empty	223	0	0
	SMCX	230	0	0
WT	Empty	219	10,500	4.79
	SMCX	296	8,250	2.78
W453R	Empty	264	469	0.18
	SMCX	259	482	0.19

*Total no. of substrate plasmids analysed
†No. of recombined substrate plasmids analysed
‡Per cent recombination = no. of recombined plasmids (*Amp*^{R}/*Cam*^{R}) / total no. of substrate plasmids (*Amp*^{R})

Figure 4 | Recognition of H3K4me3 is crucial for RAG1/2 recombinase activity *in vivo*. **a**, The H3K4me3-recognition activity of RAG2 is required for extrachromosomal V(D)J recombination *in vivo*. Left panel, western analysis of Flag-tagged full-length RAG2 proteins expressed in Br3neo human fibroblast cells confirms that wild-type (WT) and mutant RAG2 proteins are expressed at comparable levels *in vivo*. Right panel, The indicated constructs were used for transient V(D)J recombination assays in Br3neo cells. Recombination activity was normalized to wild-type activity (RAG2), which was defined as 100%. Wild-type RAG2 consistently gave recombination frequencies of ~5–6%. Results represent the mean ±s.d. of six independent experiments. **b**, Reducing H3K4 methylation levels specifically impairs V(D)J recombination by wild-type RAG2. Western analysis demonstrates that the *WDR5* shRNA vector (WDR5i) reduces H3K4me3 levels. Transient V(D)J recombination assays performed with wild-type (left graph) or mutant (right graph) RAG2 in HT1080 human fibroblast cells in the presence (stippled) or absence (filled) of a *WDR5* shRNA vector. Results represent the mean ±s.d. of six independent experiments. Table, representative recombination data. **c**, Reducing H3K4me3 levels by demethylation specifically reduces V(D)J recombination by wild-type RAG2. Western analysis confirms that SMCX expression reduces H3K4me3 levels. Transient V(D)J recombination assays were performed with wild-type (left graph) or mutant (right graph) RAG2 in Br3neo cells in the presence (hatched) or absence (filled) of SMCX. Results represent the mean ±s.d. of six independent experiments. Table, representative recombination data. **d**, The H3K4me3-recognition activity of RAG2 is required for chromosomal V(D)J recombination at the endogenous murine IgH locus. Left panel, western analysis of Flag-tagged full-length RAG2 proteins expressed in lentivirally transduced *RAG2*$^{-/-}$ Pro-B cells confirms that wild-type and mutant RAG2 proteins are expressed at comparable levels *in vivo*. Right panel, endogenous V(D)J recombination assays in Pro-B cells transduced as in the western blot. Southern blot analysis of PCR-amplified genomic DNA on an agarose gel. Serial dilutions represent PCR-amplification of 400, 200 and 100 ng of genomic DNA. Results shown are representative of four independent experiments.

M443A, and Y415A point mutations—which selectively disrupt H3K4me3-recognition—severely disrupt V(D)J recombination, complete deletion of the RAG2 C terminus (including the PHD finger) only partially compromises V(D)J recombination activity[24–27] (Supplementary Fig. 11). We propose that the RAG2–H3K4me3 interaction serves two functions: (1) increases the stable association of RAG1/2 complexes at target sites and (2) might relieve an inhibitory activity present in the C-terminal portion of RAG2 (ref. 7) (Supplementary Fig. 13). Taken together with other studies that have demonstrated a link between the writing of histone modifications and human disease[15,28,29], our results highlight the fundamental role chromatin has in human health. We postulate that, in the coming years, other naturally occurring mutations that cause inherited human diseases will be linked to disruption of lysine methylation signalling pathways.

Note added in proof: While this work was under review, another study also reported that the RAG2 PHD finger binds to methylated H3K4 (ref. 30).

METHODS SUMMARY

Biotinylated peptides were synthesized at Stanford or Yale Protein and Nucleic Acid facilities. Peptide microarray experiments were performed essentially as described[17]. Biotinylated peptide pull-down assays, calf thymus histone binding assays, and mononucleosome gel-shift assays were performed as

described[9]. Tryptophan fluorescence assays were performed essentially as described[13]. Nuclear magnetic resonance (NMR) structure determination was performed as described[7]. The structure determination is described in Methods. *In vitro* V(D)J cleavage assays were performed as described[31]. The extrachromosomal V(D)J recombination assays and the endogenous V(D)J recombination assay are described in Methods. Information about antibodies is available in Methods.

Full Methods and any associated references are available in the online version of the paper at www.nature.com/nature.

Received 24 July; accepted 2 November 2007.
Published online 21 November 2007.

1. Gellert, M. V(D)J recombination: RAG proteins, repair factors, and regulation. *Annu. Rev. Biochem.* **71,** 101–132 (2002).
2. Oettinger, M. A. How to keep V(D)J recombination under control. *Immunol. Rev.* **200,** 165–181 (2004).
3. Chowdhury, D. & Sen, R. Stepwise activation of the immunoglobulin μ heavy chain gene locus. *EMBO J.* **20,** 6394–6403 (2001).
4. Johnson, K., Angelin-Duclos, C., Park, S. & Calame, K. L. Changes in histone acetylation are associated with differences in accessibility of V_H gene segments to V-DJ recombination during B-cell ontogeny and development. *Mol. Cell. Biol.* **23,** 2438–2450 (2003).
5. Morshead, K. B., Ciccone, D. N., Taverna, S. D., Allis, C. D. & Oettinger, M. A. Antigen receptor loci poised for V(D)J rearrangement are broadly associated with BRG1 and flanked by peaks of histone H3 dimethylated at lysine 4. *Proc. Natl Acad. Sci. USA* **100,** 11577–11582 (2003).
6. Callebaut, I. & Mornon, J. P. The V(D)J recombination activating protein RAG2 consists of a six-bladed propeller and a PHD fingerlike domain, as revealed by sequence analysis. *Cell. Mol. Life Sci.* **54,** 880–891 (1998).
7. Elkin, S. K. *et al.* A PHD finger motif in the C terminus of RAG2 modulates recombination activity. *J. Biol. Chem.* **280,** 28701–28710 (2005).
8. Ragvin, A. *et al.* Nucleosome binding by the bromodomain and PHD finger of the transcriptional cofactor p300. *J. Mol. Biol.* **337,** 773–788 (2004).
9. Shi, X. *et al.* ING2 PHD domain links histone H3 lysine 4 methylation to active gene repression. *Nature* **442,** 96–99 (2006).
10. Wysocka, J. *et al.* A PHD finger of NURF couples histone H3 lysine 4 trimethylation with chromatin remodelling. *Nature* **442,** 86–90 (2006).
11. West, K. L. *et al.* A direct interaction between the RAG2 C terminus and the core histones is required for efficient V(D)J recombination. *Immunity* **23,** 203–212 (2005).
12. Li, H. *et al.* Molecular basis for site-specific read-out of histone H3K4me3 by the BPTF PHD finger of NURF. *Nature* **442,** 91–95 (2006).
13. Pena, P. V. *et al.* Molecular mechanism of histone H3K4me3 recognition by plant homeodomain of ING2. *Nature* **442,** 100–103 (2006).
14. Taverna, S. D. *et al.* Yng1 PHD finger binding to H3 trimethylated at K4 promotes NuA3 HAT activity at K14 of H3 and transcription at a subset of targeted ORFs. *Mol. Cell* **24,** 785–796 (2006).
15. Ruthenburg, A. J., Allis, C. D. & Wysocka, J. Methylation of lysine 4 on histone H3: intricacy of writing and reading a single epigenetic mark. *Mol. Cell* **25,** 15–30 (2007).
16. Ramon-Maiques, S. *et al.* The PHD finger of RAG2 recognizes histone H3 methylated at both lysine-4 and arginine-2. *Proc. Natl Acad. Sci. USA*. doi:10.1073/pnas.0709170104 (in the press).
17. Shi, X. *et al.* Proteome-wide analysis in *Saccharomyces cerevisiae* identifies several PHD fingers as novel direct and selective binding modules of histone H3 methylated at either lysine 4 or lysine 36. *J. Biol. Chem.* **282,** 2450–2455 (2007).
18. Gomez, C. A. *et al.* Mutations in conserved regions of the predicted RAG2 kelch repeats block initiation of V(D)J recombination and result in primary immunodeficiencies. *Mol. Cell. Biol.* **20,** 5653–5664 (2000).
19. Villa, A. *et al.* Partial V(D)J recombination activity leads to Omenn syndrome. *Cell* **93,** 885–896 (1998).
20. Baumann, M., Mamais, A., McBlane, F., Xiao, H. & Boyes, J. Regulation of V(D)J recombination by nucleosome positioning at recombination signal sequences. *EMBO J.* **22,** 5197–5207 (2003).
21. Sims, R. J. III & Reinberg, D. Histone H3 Lys 4 methylation: caught in a bind? *Genes Dev.* **20,** 2779–2786 (2006).
22. Iwase, S. *et al.* The X-linked mental retardation gene *SMCX/JARID1C* defines a family of histone H3 lysine 4 demethylases. *Cell* **128,** 1077–1088 (2007).
23. Perkins, E. J., Kee, B. L. & Ramsden, D. A. Histone 3 lysine 4 methylation during the pre-B to immature B-cell transition. *Nucleic Acids Res.* **32,** 1942–1947 (2004).
24. Akamatsu, Y. *et al.* Deletion of the RAG2 C terminus leads to impaired lymphoid development in mice. *Proc. Natl Acad. Sci. USA* **100,** 1209–1214 (2003).
25. Corneo, B. *et al.* Rag mutations reveal robust alternative end joining. *Nature* **449,** 483–486 (2007).
26. Kirch, S. A., Rathbun, G. A. & Oettinger, M. A. Dual role of RAG2 in V(D)J recombination: catalysis and regulation of ordered Ig gene assembly. *EMBO J.* **17,** 4881–4886 (1998).
27. Liang, H. E. *et al.* The ''dispensable'' portion of RAG2 is necessary for efficient V-to-DJ rearrangement during B and T cell development. *Immunity* **17,** 639–651 (2002).
28. Shi, Y. & Whetstine, J. R. Dynamic regulation of histone lysine methylation by demethylases. *Mol. Cell* **25,** 1–14 (2007).
29. Tenney, K. & Shilatifard, A. A. COMPASS in the voyage of defining the role of trithorax/MLL-containing complexes: linking leukemogensis to covalent modifications of chromatin. *J. Cell. Biochem.* **95,** 429–436 (2005).
30. Liu, Y., Subrahmanyam, R., Chakraborty, T., Sen, R. & Desiderio, S. A plant homeodomain in Rag-2 that binds hypermethylated lysine 4 of histone H3 is necessary for efficient antigen-receptor-gene rearrangement. *Immunity* **4,** 561–571 (2007).
31. Matthews, A. G., Elkin, S. K. & Oettinger, M. A. Ordered DNA release and target capture in RAG transposition. *EMBO J.* **23,** 1198–1206 (2004).

Supplementary Information is linked to the online version of the paper at www.nature.com/nature.

Acknowledgements We thank K.-J. Armache and J.-J. Song for the generous gift of recombinant mononucleosomes; R. Kingston and members of the Kingston laboratory for helpful discussions; and N. Lau, J.-J. Song, and M. Gellert for critical reading of this manuscript. This work was supported by NIH grants (M.A.O., O.G., D.I. and T.G.K.), as well as a Korea Research Foundation grant (S.H.). O.G. is a recipient of a Burroughs Wellcome Career Award in Biomedical Sciences and a Kimmel Scholar Award. S.R.-M. has been the recipient of a fellowship from the Human Frontier Science Program. A.J.K. is funded by Stanford University through a Genentech Foundation Predoctoral Fellowship. A.G.W.M. is a Howard Hughes Medical Institute Predoctoral Fellow.

Author Information Reprints and permissions information is available at www.nature.com/reprints. Correspondence and requests for materials should be addressed to M.A.O. (oettinger@frodo.mgh.harvard.edu) or O.G. (ogozani@stanford.edu).

METHODS

Materials and plasmids. Antibodies used in the study were: anti-Histone H3 (Abcam); anti-Flag M5 (Sigma); anti-Flag M2 (Sigma); anti-glutathione *S*-transferase (GST; Santa Cruz); donkey anti-rabbit IgG HRP-linked F(ab')$_2$ fragment (GE Healthcare); sheep anti-mouse IgG HRP-linked whole antibody (GE Healthcare); and Alexa Fluor 647 chicken anti-rabbit IgG (Invitrogen). GST–RAG2$_{PHD}$ (amino acids 414–487), GST–RAG2$_{PHD}$ (amino acids 414–527) and Flag-tagged RAG2 were described previously[7]. Point mutations were generated by site-directed mutagenesis PCR using Pfu turbo DNA polymerase (Stratagene). The GST–PHD finger of hING2 (amino acids 200–281) was described previously[9].

Peptide microarray. Peptide microarray experiments were performed as described previously[17]. Briefly, biotinylated histone peptides were printed in six replicates onto a streptavidin-coated slide (ArrayIt) using a VersArray Compact Microarrayer (Bio-Rad). After a short blocking incubation with biotin (Sigma), the slides were incubated with GST-fused RAG2$_{PHD}$ in peptide binding buffer (50 mM Tris-HCl, pH 7.5, 150 mM NaCl, 0.1% Nonidet P-40, 20% fetal bovine serum) overnight at 4 °C with gentle agitation. After washing with the same buffer, slides were probed first with anti-GST antibody and then fluorescein-conjugated secondary antibody and visualized with a GenePix 4000 scanner (Molecular Devices).

Biotinylated-peptide binding assays. Biotinylated-peptide pull-down assays were performed as described previously[9]. Briefly, 1 μg of biotinylated peptides were incubated with 1 μg of GST–PHD-fingers in peptide binding buffer (50 mM Tris-HCl, pH 7.5, 300 mM NaCl, 0.1% Nonidet P-40) overnight at 4 °C. After 1 h incubation with streptavidin beads (Amersham), complexes were washed 3 times with the binding buffer, and the bound proteins were subjected to either western or Coomassie analysis.

Calf thymus histone binding assays. Calf thymus histone binding assays were performed as described previously[9]. Briefly, 10 μg of GST–RAG2$_{PHD}$ was incubated with 25 μg of calf thymus histones (Worthington) in binding buffer (50 mM Tris-Hcl, pH 7.5, 1 M NaCl, 1% Nonidet P-40) overnight at 4 °C. After being incubated with glutathione beads for 1 h, complexes were washed 3 times with binding buffer, and bound proteins were subjected to western analysis.

Mononucleosome shift assay. Mononucleosome gel-shift assays were performed as described previously[9]. Briefly, 1.5 μg of mononucleosomes isolated from HeLa cells or assembled from recombinant histones[32] were incubated with GST–RAG2$_{PHD}$ in binding buffer (20 mM HEPES, pH 7.9, 80 mM KCl, 0.1 mM, $ZnCl_2$, 0.1% EDTA and 10% glycerol) at 30 °C for 30 min. The reaction was then subjected to 5% TBE native gel electrophoresis and visualized with ethidium-bromide staining.

Tryptophan fluorescence spectroscopy. The fluorescence spectra were recorded at 25 °C on a Fluoromax3 spectrofluorometer. The samples of 10 μM RAG2$_{PHD}$ containing progressively increasing concentrations (up to 2 mM) of histone H3 peptides (amino acids 1–12) were excited at 295 nm. Emission spectra were recorded between 305 and 405 nm with a 0.5-nm step size and a 1-s integration time and averaged over 3 scans. The K_ds were determined by a non-linear least-squares analysis using the equation: $\Delta I = (\Delta I_{max} * L)/(K_D + L)$, where L is concentration of the histone peptide, ΔI is observed change of signal intensity, and ΔI_{max} is the difference in signal intensity of the free and bound states of the RAG2 PHD finger. The K_d value was averaged over two experiments for the H3K4me3 binding and over three separate experiments for the binding of H3K4me0, H3K4me1 and H3K4me2 peptides.

Data collection and structure determination. The RAG2 PHD finger (amino acids 414–487) was prepared as described[16]. Crystals of its complex with H3K4me3 were obtained at 3 mg ml^{-1} protein concentration and 1:1.5 molar ratio of protein to peptide with a precipitant solution of 26% PEG 3350 and 0.18 M potassium thiocyanate. X-ray diffraction data were collected from a single crystal of RAG2$_{PHD}$– H3K4me3 complex on a Mar225 charge-coupled device detector at ID-22 1 Å beamline in Advanced Photon Source (APS) at −160 °C. The crystal belongs to the C2 space group with 2 RAG2$_{PHD}$–H3K4me3 complexes per asymmetric unit (Supplementary Table 1). Ramachandran statistics: 93.3% allowed region, 6.7% additionally allowed region. The data set was processed and scaled at 1.15 Å using HKL2000 (ref. 33). Crystallographic phases were obtained by molecular replacement with PHASER[34], using as a model the 2.4 Å resolution structure of RAG2$_{PHD}$–H3K4me3 determined previously[16]. The model was traced using COOT[35] and refined using CNS[36] and SHELX[37]. Individual anisotropic displacement parameters were refined for all atoms, and hydrogens were added in the late stages of refinement.

***In vitro* V(D)J cleavage assays.** Flag-tagged RAG2 and derivatives were used for *in vitro* V(D)J cleavage assays as described previously[38]. Briefly, V(D)J cleavage assays were initiated by the addition of R1 (~80 ng) and R2 (~10 ng) proteins to a 10 μl reaction mixture containing 0.25 pmol of ^{32}P-labelled, uncleaved 12-RSS substrate (VDJ100/101) in 60 mM K-glutamate, 1 mM $MnCl_2$, 25 mM Hepes, pH 7.5, and 2mM DTT. After a 2 h incubation at 30 °C, the reactions were stopped by addition of 95% formamide loading dye. The samples were denatured by heating at 95 °C for 5 min, and reaction products were visualized by autoradiography of samples separated by denaturing electrophoresis.

Extrachromosomal V(D)J recombination assays. Extrachromosomal V(D)J recombination assays were performed as described previously[39] in either Br3neo[39] or HT1080[9] human fibroblastoid cells, and the plasmid pGG49 was used as the reporter[40]. Full-length RAG1 was transiently expressed using the pcDNA6-myc-hisA vector (Invitrogen). RAG2 and derivatives were transiently expressed using the p3xFLAG-CMV vector (Sigma). Expression of all proteins was confirmed by western analysis. For the *WDR5* shRNA experiments, HT1080 cells were first stably transfected with either a *WDR5* shRNA vector or a control vector that lacks the shRNA insert. These cells were subsequently transfected with *RAG1*, *RAG2* and a recombination substrate. Activity was normalized to that of wild-type RAG2 in the absence of WDR5, which was defined as 100%. For the SMCX experiments, Br3neo cells were simultaneously co-transfected with *RAG1*, *RAG2*, a recombination substrate, and either an *SMCX* mammalian expression vector, or a control vector that lacks the *SMCX* insert. Activity was normalized to that of wild-type RAG2 in the absence of SMCX, which was defined as 100%.

Endogenous V(D)J recombination assays. Endogenous V(D)J recombination assays were performed essentially as described previously[26,41], except that *RAG2*$^{-/-}$ Pro B cells were lentivirally transduced with *RAG2* and derivatives. Expression of all proteins was confirmed by western analysis.

32. Luger, K., Mader, A. W., Richmond, R. K., Sargent, D. F. & Richmond, T. J. Crystal structure of the nucleosome core particle at 2.8 A resolution. *Nature* **389**, 251–260 (1997).
33. Ottinowski, Z. & Minor, W. Processing of X-ray diffraction data collected in oscillation mode. *Methods Enzymol.* **276**, 307–326 (1997).
34. McCoy, A. J. Solving structures of protein complexes by molecular replacement with Phaser. *Acta Crystallogr. D Biol. Crystallogr.* **63**, 32–41 (2007).
35. Emsley, P. & Cowtan, K. Coot: model-building tools for molecular graphics. *Acta Crystallogr. D* **60**, 2126–2132 (2004).
36. Brunger, A. T. *et al.* Crystallography & NMR system: A new software suite for macromolecular structure determination. *Acta Crystallogr. D* **54**, 905–921 (1998).
37. Sheldrick, G. M. & Schneider, T. R. SHELXL: High-resolution refinement. *Methods Enzymol.* **277**, 319–343 (1997).
38. Elkin, S. K., Matthews, A. G. & Oettinger, M. A. The C-terminal portion of RAG2 protects against transposition *in vitro*. *EMBO J.* **22**, 1931–1938 (2003).
39. Dai, Y. *et al.* Nonhomologous end joining and V(D)J recombination require an additional factor. *Proc. Natl Acad. Sci. USA* **100**, 2462–2467 (2003).
40. Gauss, G. H. & Lieber, M. R. Unequal signal and coding joint formation in human V(D)J recombination. *Mol. Cell. Biol.* **13**, 3900–3906 (1993).
41. Schlissel, M. S., Corcoran, L. M. & Baltimore, D. Virus-transformed pre-B cells show ordered activation but not inactivation of immunoglobulin gene rearrangement and transcription. *J. Exp. Med.* **173**, 711–720 (1991).